

Article

# Re-188 Enhances the Inhibitory Effect of Bevacizumab in Non-Small-Cell Lung Cancer

Jie Xiao <sup>1,2,†</sup>, Xiaobo Xu <sup>3,†</sup>, Xiao Li <sup>1,2</sup>, Yanli Li <sup>1,2</sup>, Guobing Liu <sup>1,2</sup>, Hui Tan <sup>1,2</sup>, Hua Shen <sup>4</sup>, Hongcheng Shi <sup>1,2</sup> and Dengfeng Cheng <sup>1,2,\*</sup>

<sup>1</sup> Department of Nuclear Medicine, Zhongshan Hospital, Fudan University, Shanghai 200032, China; xiaojie\_fdu@163.com (J.X.); leelobster@126.com (X.L.); drliyanli@163.com (Y.L.); liuguobing0422@163.com (G.L.); 13818914579@163.com (H.T.); shihongcheng163@163.com (H.S.)

<sup>2</sup> Shanghai Institute of Medical Imaging, Shanghai 200032, China

<sup>3</sup> Departments of Respiratory Medicine, Zhongshan Hospital, Fudan University, Shanghai 200032, China; xu.xiaobo@zs-hospital.sh.cn

<sup>4</sup> Institute of Applied Physics, Chinese Academy of Sciences, Shanghai 200032, China; shenhua@sinap.ac.cn

\* Correspondence: cheng.dengfeng@zs-hospital.sh.cn Tel.: +86-21-64041990

† These authors contributed equally to this work.

Academic Editor: Zhen Cheng

Received: 18 July 2016; Accepted: 25 September 2016; Published: 30 September 2016

**Abstract:** The malignant behaviors of solid tumors such as growth, infiltration and metastasis are mainly nourished by tumor neovascularization. Thus, anti-angiogenic therapy is key to controlling tumor progression. Bevacizumab, a humanized anti-vascular endothelial growth factor (VEGF) antibody, plus chemotherapy or biological therapy can prolong survival for cancer patients, but treatment-related mortality is a concern. To improve inhibitory effect and decrease side-effects on non-small-cell lung cancer (NSCLC), we used Re-188, which is a  $\beta$  emitting radionuclide, directly labeled with bevacizumab for radioimmunotherapy in a human A549 tumor model. Cytotoxic assay data showed that, after  $^{188}\text{ReO}_4^-$  or  $^{188}\text{Re}$ -bevacizumab at different concentration for 4 and 24 h, a time- and radioactivity does-dependent reduction in cell viability occurred. Also, an apoptosis assay conformed great apoptosis in the  $^{188}\text{Re}$ -bevacizumab group compared with controls and other treatment groups. In vivo, tumor volumes in the  $^{188}\text{Re}$ -bevacizumab (11.1 MBq/mice) group were not reduced but growth was delayed compared with other groups. Thus,  $^{188}\text{Re}$ -bevacizumab enhanced the therapeutic effect of bevacizumab, suggesting a potential therapeutic strategy for NSCLC treatment.

**Keywords:** bevacizumab; non-small cell lung cancer; radioimmunotherapy; Re-188; Tc-99m

## 1. Introduction

Lung cancer is the leading cause of cancer death worldwide and represents a significant financial and social burden [1]. Non-small-cell lung cancer (NSCLC), the mostly common cancer subtype, accounts for 85% of all new lung cancer diagnoses [2]. Due to late onset of clinical manifestations, patients are commonly diagnosed at advanced or inoperable-stages. Recently, chemotherapy with platinum plus one other anti-tumor agents is recommended for first-line chemotherapy, but side-effects are a concern [3]. Although maintenance therapy followed by second-line cytotoxic chemotherapy is common, advanced stage patients did not live one year beyond median survival [4]. Thus, effective, low side-effect therapeutic methods for NSCLC treatment are needed.

Tumor progression (growth, infiltration and metastasis) are reportedly supported by tumor neovascularization. Thus, tumor angiogenesis is thought to be an approach for treating cancers [5,6]. Bevacizumab, a humanized monoclonal antibody (MAb), that specifically binds to vascular endothelial

growth factor (VEGF) and can block neovascularization, was approved by the FDA [7]. In randomized clinical trials, survival benefits were improved when bevacizumab was added to standard chemotherapy regimens to treat metastatic colorectal cancer and advanced NSCLC [7,8]. Radioimmunotherapy (RIT) is an alternative for patients with advanced cancers. Using selective targeting to cancer-associated antigens on the tumor-cell surface, monoclonal antibody-mediated radionuclide can deliver high-dose therapeutic radiation to cancer cells with minimal exposure of normal cells [9–11]. The first radiolabeled antibody for anti-tumor therapy,  $^{90}\text{Y}$ -murine anti-CD20 antibody, ibritumomab, offered a satisfactory therapeutic response, and was approved for clinical practice in 2002 [12]. Coupled to  $^{131}\text{I}$ , tositumomab has been used to treat chronic lymphocytic leukemia or small lymphocytic lymphoma in first remission. Also, patients with leukemias or lymphomas enjoyed more survival benefits from RIT than without RIT treatment [13–15]. However, for solid tumor, which are radio-resistant and less accessible to MAbs, a concern remains about limited clinical efficacy [16].

According to Lucas,  $^{90}\text{Y}$  and  $^{188}\text{Re}$  were regarded as the best candidates for solid tumor treatment such as for NSCLC [17]. In addition, considering the appropriate half-life of 16.9 h (0.7 d), therapeutic beta radiation ( $E\beta = 2.118\text{ Mev}$ ) and easy used in-home,  $^{188}\text{Re}$  was selected as the radioisotope for RIT in this study. The radiotherapeutic agent  $^{188}\text{Re}$ -bevacizumab was designed, and its therapeutic efficacy was evaluated in tumor models of NSCLC.

## 2. Results and Discussion

### 2.1. Radiolabeling

The synthesis of  $^{188}\text{Re}$ -bevacizumab was achieved by a two-step reaction (Figure 1A). For paper chromatography studies, the  $R_f$  values of radiolabeled bevacizumab and  $^{188}\text{Re}$ -colloid were 0.0–0.1, and the  $R_f$  value of free or unbound  $^{188}\text{ReO}_4^-$  was 0.8–0.9 in normal saline. In contrast, for the mixed solvent system  $V_{\text{ethanol}}:V_{\text{ammonia}}:V_{\text{water}} = 2:5:1$  the  $R_f$  value of radiolabeled bevacizumab and free  $^{188}\text{ReO}_4^-$  were 0.8–0.9, and the  $R_f$  value of radiolabeled bevacizumab and  $^{188}\text{Re}$ -colloid were 0.0–0.1. Thus, yields of  $94.5\% \pm 1\%$  were calculated for unbound  $^{188}\text{ReO}_4^-$  and less than 2% radiocolloidal under these conditions: 100  $\mu\text{g}$  (1 mg/mL) of bevacizumab was incubated with  $^{188}\text{ReO}_4^-$  (37–74 MBq) in acetic acid buffer solution (pH = 4.5) for 30 min at room temperature (RT). Purification was performed with disposable G25 PD-10 desalting columns (GE Healthcare Bio-Sciences Corp., Piscataway, NJ, USA) and a radiochemical purity of more than 98% was achieved. After purification, radiolabeled products were used for studies.

In this present study, the influence on radiolabeling efficiency by pH was also investigated. The optimal pH value was 4.5, as the results in Figure 1A. According to the published literature [18–20], the direct radiolabeling of  $^{188}\text{Re}$  to antibodies occurs within a pH range from 4 and 6, and it is proposed that a radiolabeling pH value lower than 4 could compromise the immunoreactivity of the antibodies, while a higher pH value increases the percentage of unbound  $^{188}\text{ReO}_4^-$ .

### 2.2. Stability in Vitro

After purification,  $^{188}\text{Re}$ -bevacizumab was diluted and incubated in mouse serum and normal saline (1:5 and 1:1, respectively). Radiolabeling was measured at 4, 12 and 24 h at 37 °C (Figure 1C). After 12 h of incubation, over than 95% of labelled products remained intact in both normal saline and serum. For 24 h, less than 10% decomposition was observed in mouse serum, suggesting a favorable stability in vitro.

### 2.3. Cytotoxicity Assay (CCK-8)

Cell viability of all treated groups at different times points is shown in Figure 2, where the data show that the viability was time- and dose- or radioactive dose-dependent. Cells incubated with fresh medium were the most viable, whereas  $^{188}\text{Re}$ -bevacizumab (1.85 MBq) treatment reduced viability the most.

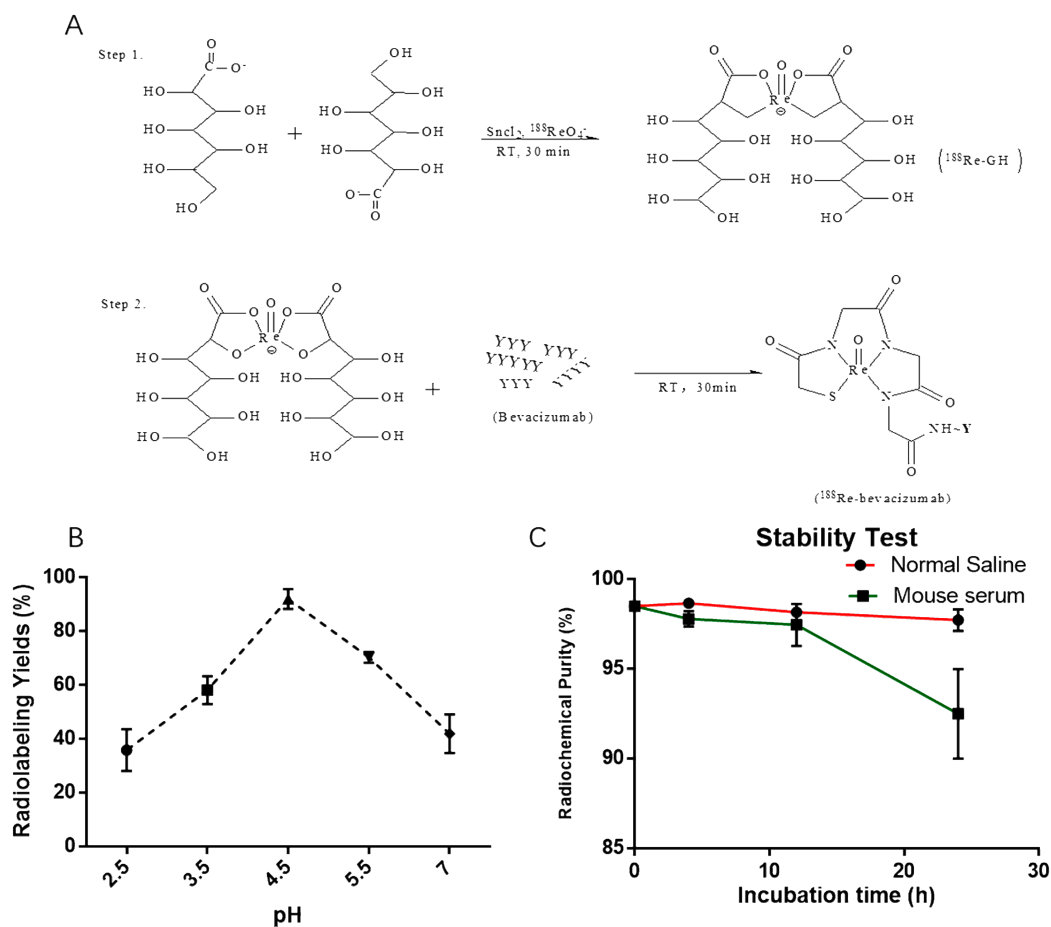


**Figure 1.** (A) Synthesis of  $^{188}\text{Re}$ -bevacizumab by a two-step reaction; (B) Effects of pH on complexation yield of  $^{188}\text{Re}$ -bevacizumab; (C) Stability of  $^{188}\text{Re}$ -bevacizumab incubated with normal saline (pH 7.4) and mouse serum in vitro at room temperature was measured at various times.

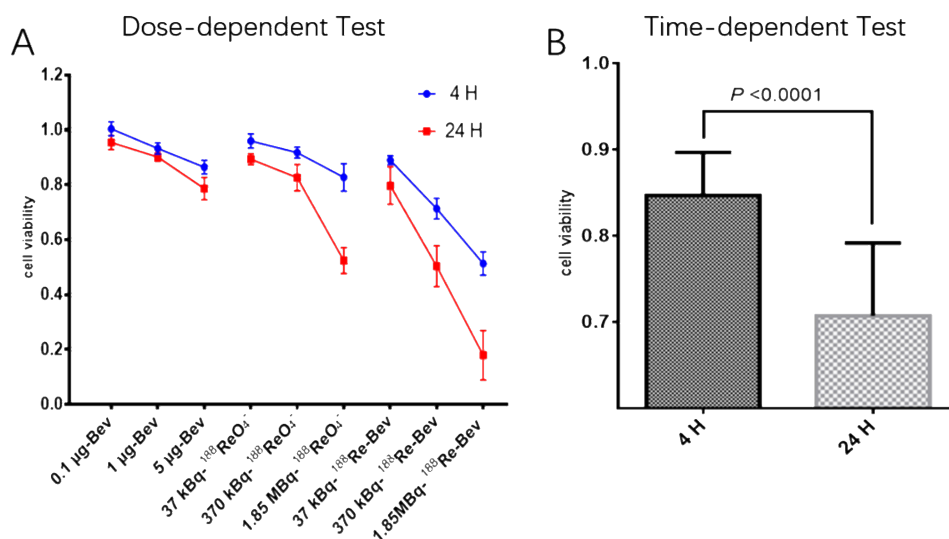


**Figure 2.** Cell viability is in a radioactive- and time-dependent manner. (A) Dose-dependent test: changes of cell viability after incubation with fresh medium containing bevacizumab at various concentrations, free  $^{188}\text{Re}$  and  $^{188}\text{Re}$ -bevacizumab; (B) Time-dependent test: compared average cell viability of all treated group (bevacizumab, free  $^{188}\text{Re}$  and  $^{188}\text{Re}$ -bevacizumab) at 4 h and at 24 h.

Increasing the radioactivity dose from 37 kBq to 1.85 MBq proportionally decreased cell viability at 4 h and 24 h in all groups. Thus, A549 cells are more sensitive to  $^{188}\text{Re}$ -bevacizumab compared to bevacizumab alone at equal concentration. How bevacizumab inhibits cell growth is unknown, but Wang suggested that cytotoxicity in tumor cells after bevacizumab administration may be due to endoplasmic reticulum stress, which accelerates apoptosis, or autocrine VEGF [21].

#### 2.4. Apoptosis Assay

Viable cells were identified as PE-Annexin V<sup>-</sup> and 7-AAD<sup>-</sup> (lower left quadrants, Q4) and PE-Annexin V<sup>-</sup> and 7-AAD<sup>+</sup> (upper left quadrants, Q1) were necrotic. Early apoptotic cells were PE-Annexin-V<sup>+</sup> and 7-AAD<sup>-</sup> (lower right quadrants, Q3), while PE-Annexin-V<sup>+</sup> and 7-AAD<sup>+</sup> (upper right quadrants, Q2) were late apoptotic cells. The percentages of early apoptotic cells and late apoptotic cells from each group appear in Figure 3. Compared with controls (4.02% ± 1.05%), apoptosis increased after bevacizumab treatment,  $^{188}\text{ReO}_4^-$  (370 kBq /mL), and  $^{188}\text{Re}$ -bevacizumab (370 kBq/μg/mL).

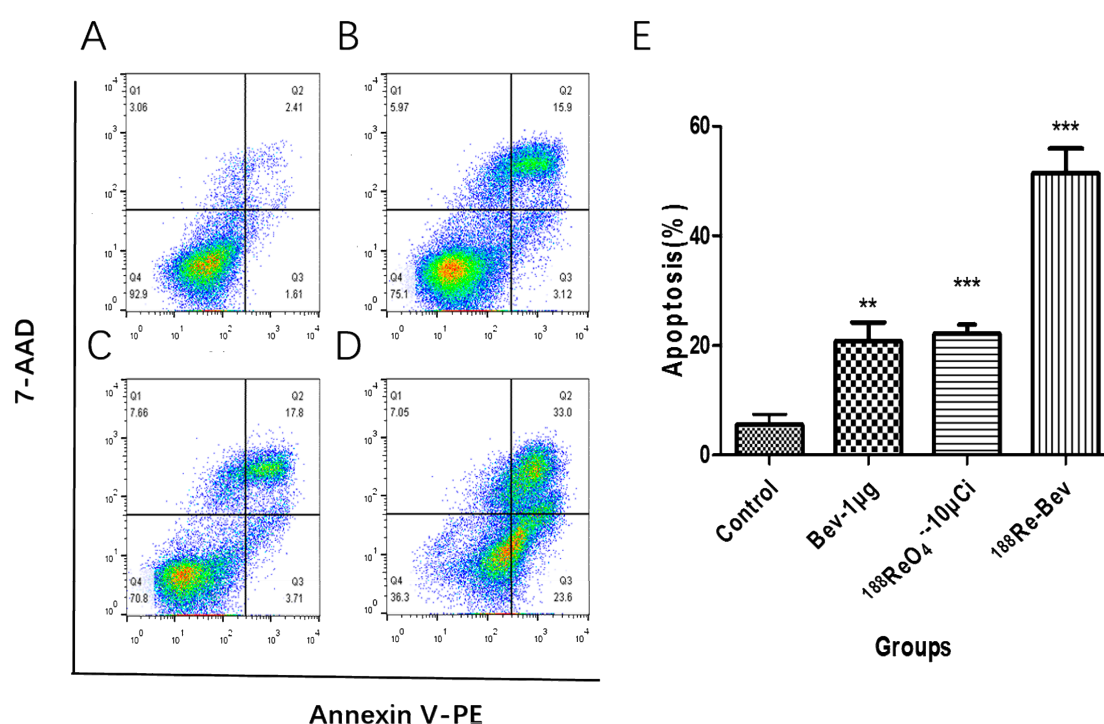


**Figure 3.** The percentage of apoptotic cells, inducing by bevacizumab (B); unbound  $^{188}\text{ReO}_4^-$  (C) and  $^{188}\text{Re}$ -bevacizumab (D) at equal concentration or radioactivity, untreated group as control (A). (E) The combined pro-apoptotic efficiency of  $^{188}\text{Re}$ -bevacizumab is greater than the sum if each agent used along. \*\*  $p < 0.01$ ; \*\*\*  $p < 0.001$ .

#### 2.5. Micro SPECT/CT Imaging

To eliminate the influence on therapeutic efficiency by  $^{188}\text{ReO}_4^-$  before and after treatment,  $^{99\text{m}}\text{Tc}$ -MAG<sub>3</sub>-bevacizumab was used to monitor angiogenic changes during treatment. Whole body images and relevant axial slices of pre- and post-therapy A549 xenograft mouse treated with  $^{188}\text{Re}$ -bevacizumab are depicted in Figure 4. Images acquired at 4 h after injection showed intense uptake of drug by lung, liver, spleen, kidney and bladder. Tumor uptake before treatment was more intensive than post-treatment, suggesting effective anti-angiogenic efficacy of  $^{188}\text{Re}$ -bevacizumab, and treatment was ceased. Bevacizumab has a long half-life and binds to VEGF-A, a key mediator of angiogenesis [22]. Thus, the accumulation of  $^{99\text{m}}\text{Tc}$ -MAG<sub>3</sub>-bevacizumab in organs may be explained by organ mesenchyme secretion of VEGF [23].



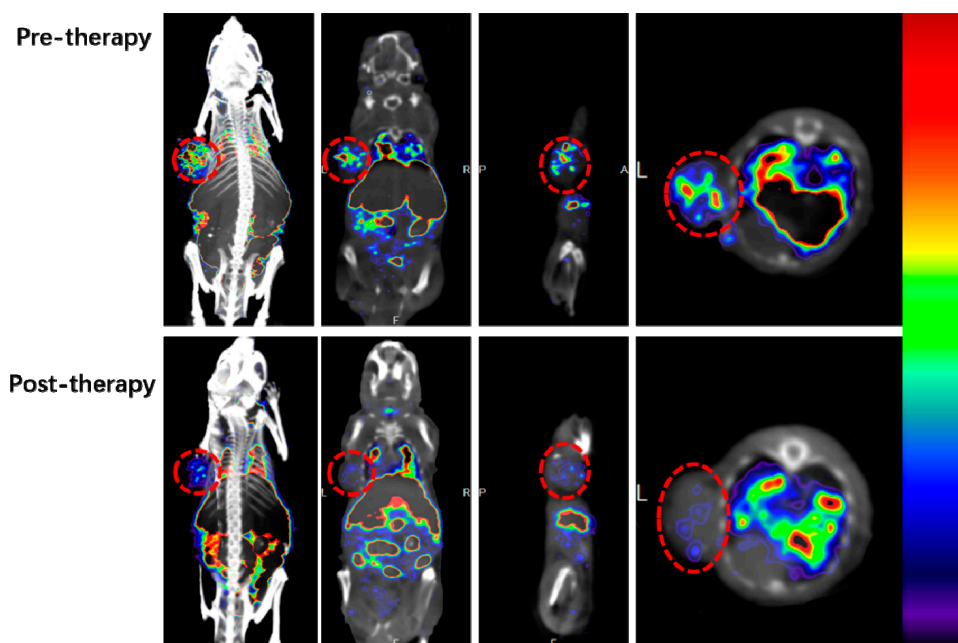


**Figure 4.** Maximum Intensity Projection (MIP) images and its axial, transverse and sagittal images demonstrate that  $^{99m}\text{Tc}$ -bevacizumab uptake in tumor are less than pre-therapy.

## 2.6. Assessment of Treatment Effect in Vivo

Bevacizumab (1.5 mg/kg or 30  $\mu\text{g}$  per mice) and  $^{188}\text{Re}$ -bevacizumab (11.1 MBq/30  $\mu\text{g}$  per mice) were separately injected into the tail vein treatment groups weekly and tumor sizes and body weight were recorded (Figure 5).

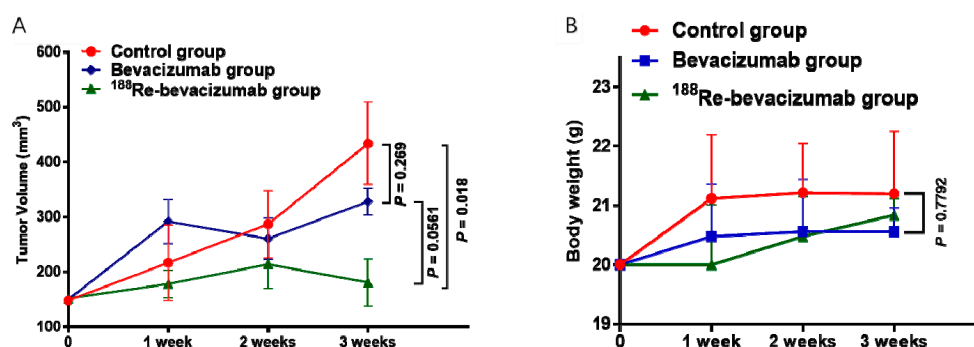


**Figure 5.** The alteration of tumor volumes and body weight. (A) Tumor volume are effectively inhibited in  $^{188}\text{Re}$ -bevacizumab group; (B) No significant weight loss is occurred in  $^{88}\text{Re}$ -bevacizumab group.

Compared with controls, tumor growth in the  $^{188}\text{Re}$ -bevacizumab and bevacizumab treatment groups were obviously delayed with no significant regression ( $p$  value = 0.018 < 0.05). Although there was no statistical difference ( $p$  value = 0.0561 > 0.05) between the  $^{188}\text{Re}$ -bevacizumab treatment group and the bevacizumab treatment group, more pronounced inhibition was observed in the  $^{188}\text{Re}$ -bevacizumab treatment group. According to a previous report [24], dosimetry analyses of  $^{177}\text{Lu}$ -DOTA-RS7 showed that complete remissions were obtained in the maximal tolerated dose group in tumor-bearing nude mice. Thus, in order to gain more benefit from  $^{188}\text{Re}$ -bevacizumab treatment, dosimetry analyses will be performed in our future work. Animal weight gain one week after treatment in the treatment groups was slowed and food intake was less, but these differences were not statistically different ( $p$  value = 0.7792 > 0.05).

Effective radiotherapy requires maximum therapeutic radioactivity accumulation in tumors and long-time retention. Micro SPECT/CT images show that  $^{99m}\text{Tc}$ -bevacizumab was taken up by tumors and cleared slowly. Similarly characteristics of bevacizumab permit the delivery of a high-dose  $^{188}\text{Re}$  to tumor tissues and minimizes exposure of normal tissue.

### 3. Experimental Section

#### 3.1. Materials and Reagents

Solvents and reagents used in radiolabeling reactions were of analytical grade, used without any further purification and purchased from Sigma-Aldrich (St. Louis, MO, USA), BD Biosciences (New York, NJ, USA). Bevacizumab (Avastin) was from Roche Pharma Ltd. (Basel, Switzerland).

$^{188}\text{Re}$  was obtained as its perrhenate by elution from an alumina-column-based  $^{188}\text{W}/^{188}\text{Re}$  generator with normal saline (LaiTai Biotechnology, Jiangsu, China).  $\text{Na}^{99m}\text{TcO}_4$  was supplied by Shanghai GMS Pharmaceutical Co., Ltd. (Shanghai, China). Flexible silica gel 60 F254 plates was purchased from Merck (Darmstadt, Germany) and used for thin-layer chromatography (TLC) studies. Micro SPECT/CT imaging was performed with a Nano SPECT/CT scanner (Mesido, Budapest, Hungary) at the Cancer Center of Shanghai.

Human lung A549 adenocarcinoma cells were purchased from the Chinese Type Culture Collection (Chinese Academy of Sciences, Shanghai, China). Male nude mice (4–6 weeks-old, 20–25 g) obtained from Slac Biotechnology (Shanghai, China) which were bred in a SPF laboratory animal facility at Fudan University were used as xenograft models. All animal experiments were conducted in accordance with relevant guidelines and regulations, and were approved by the Institutional Animal Care and Committee of Fudan University.

#### 3.2. Radiolabeling and Stability in Vitro

##### 3.2.1. Radiolabeling

Bevacizumab, monoclonal antibody, was directly labeled with  $^{188}\text{ReO}_4^-$  by ligand exchange using  $^{188}\text{Re}$ -glucoheptonate according to a published method [25,26]. Briefly, 100–200  $\mu\text{L}$  of  $^{188}\text{ReO}_4^-$  fresh perrhenate eluate (185–370 MBq) in normal saline were added to a solution containing 10 mg of sodium  $\alpha$ -D-glucoheptonate dihydrate (dissolved in acetic acid, pH value of 2.5–7, 0.1 M), and treated with  $\text{SnCl}_2$  (range 200–1500  $\mu\text{g}$ ) as reductant at room temperature for 30 min. The  $^{99m}\text{Tc}$ -MAG<sub>3</sub>-bevacizumab radioproduct was synthesized according to described procedures [27,28].

##### 3.2.2. Stability Study in Vitro

To estimate the stability of  $^{188}\text{Re}$ -bevacizumab in vitro, a sample (10  $\mu\text{L}$ ) from the final preparation was incubated in normal saline (10  $\mu\text{L}$ ) and diluted in mice serum (50  $\mu\text{L}$ ) at 4 h, 12 h and 24 h at 37 °C. The analysis was repeated three times.

Labeling efficiency and stability was measured by spotting samples on BSA blocked instant thin-layer chromatography silica gel (ITLC-SG). When the eluent of normal saline reached the front, the strip was removed, dried and cut into 1-cm sections and counted. All radioactive measurements were conducted on a gamma radioimmunoassay counter (GC-1200, Zhongjia Co., Ltd., Hefei, China). Radiolabeling of  $^{188}\text{Re}$ -bevacizumab = 100% – colloidal (%) – unbound  $^{188}\text{ReO}_4^-$  (%).

#### 3.3. Cytotoxicity Assay (CCK-8)

The human adenocarcinoma A549 cell line was cultured in Dulbecco's Modified Eagle Media (DMEM) or RPMI-1640 medium supplemented with 10% fetal bovine serum (Gibco, Life Tech, Grand Island, NE, USA), 2 mM L-glutamine, penicillin (100 IU/mL) and streptomycin (100  $\mu\text{g}/\text{mL}$ ) in a humidified atmosphere of air containing 5%  $\text{CO}_2$  at 37 °C. A549 cells cultured at the logarithmic growth phase were passaged or stored at 1:3 ratios. All experiments were performed between passages 3 and 5.

Cytotoxicity of  $^{188}\text{Re}$ -bevacizumab was evaluated with a cell count kit-8 (CCK-8) according to the manufacturer's instruction. A549 cells were trypsinized and suspended at a concentration of  $5 \times 10^4/\text{mL}$  and when they reached 80% confluence,  $5 \times 10^3$  cell were seeded and cultured with 100  $\mu\text{L}$  complete medium with 10% FBS in 96-well plates coated with 0.05% rat tail collagen. After culturing for 24 h, medium was removed and replaced with 100  $\mu\text{L}$  fresh medium containing bevacizumab at different concentrations,  $^{188}\text{Re}$  (1, 10, 50  $\mu\text{Ci}/\text{mL}$ ) and equal amounts of  $^{188}\text{Re}$ -bevacizumab. A 549 cells were incubated in each desired medium as stated above for 4 h and 24 h. To evaluate cell viability, 10  $\mu\text{L}$  of CCK-8 solution was added to each well, and 96-well plates were continuously incubated at 37 °C for 2 h. The OD values were read at 450 nm to measure cell viability as following: cell viability (%) = [OD (treated group) – OD (blank)] / [OD (control group) – OD (blank)]  $\times$  100%.

### 3.4. Apoptosis Assay

An apoptosis kit (FITC Annexin V Apoptosis Detection Kit) was used to measure apoptotic and necrotic cells. According to the manufacturer's instructions, A549 cells were seeded in 25  $\text{cm}^2$  plastic flasks and incubated for 48 h. Then, cells were treated with bevacizumab (1  $\mu\text{g}$ ),  $^{188}\text{Re}$  (370 kBq or 10  $\mu\text{Ci}$ ),  $^{188}\text{Re}$ -bevacizumab (10  $\mu\text{Ci}$ -1  $\mu\text{g}$ ), meanwhile, cells incubated with fresh medium were controls. Next, 24 h later, cells were collected, washed twice with cold PBS, and then re-suspended and diluted in 1  $\times$  binding buffer ( $1 \times 10^6/\text{mL}$ ). Then,  $1 \times 10^5$  cells (100  $\mu\text{L}$ ) were stained with PE-Annexin V (5  $\mu\text{L}$ ) and 7-AAD (5  $\mu\text{L}$ ) and incubated for 15 min at room temperature in the dark. Experiments were performed in triplicate.

### 3.5. Tumor Xenografts and Treatment Design

Tumor xenografts were established in nu/nu male mice via injection of approximately  $6 \times 10^6$  A549 cells in the left shoulder area. When tumor volumes reached 150  $\text{mm}^3$ , mice were randomly divided into three groups of fifteen animals as follows: controls, bevacizumab treated, and  $^{188}\text{Re}$ -bevacizumab treated. Furthermore, A549 tumor models were treated weekly for three weeks as follows: (1) normal saline every week (control group, 100  $\mu\text{L}$  i.v.); (2) bevacizumab (1.5 mg/kg/week, 100  $\mu\text{L}$ , i.v.); (3)  $^{188}\text{Re}$ -bevacizumab (11.1 MBq/week/mouse, 100  $\mu\text{L}$ , i.v.); Tumor volumes and animal weights were recorded weekly. Tumor volumes were estimated using the equation of  $0.5 \times \text{length} \times (\text{width})^2$ . All animals were observed daily to assess general health.

### 3.6. Micro SPECT/CT Imaging

Micro-SPECT/CT imaging was following the described method [29] in three mice before the initial treatment with  $^{188}\text{Re}$ -bevacizumab and after final treatment at 3 weeks.  $^{99\text{m}}\text{Tc}$ -MAG<sub>3</sub>-bevacizumab (500  $\mu\text{Ci}/50 \mu\text{g}/\text{mice}$ ) was injected, and then CT and SPECT imaging was performed 4 h later.

## 4. Conclusions

$^{188}\text{Re}$ -bevacizumab offered high yield with direct labeling and had favorable stability in vitro.  $^{188}\text{Re}$ -bevacizumab enhanced tumor inhibition for NSCLC in both in vivo and in vitro studies.

**Acknowledgments:** This work was funded in part by the National Natural Science Foundation of China (No. 81471706 and 81201130) and Shanghai Municipal Commission of Health and Family Planning (XYQ2013106). We thank Kui Chen (Jiangsu LaiTai Medical Biotechnology Inc.) for helping with Re-188 elution. We also thank Jianping Zhang and Yingjian Zhang at the Center for Biomedical Imaging, Fudan University and Shanghai Engineering Research Center of Molecular Imaging Probes for SPECT/CT imaging.

**Author Contributions:** Jie Xiao and Dengfeng Cheng wrote and edited the main manuscript text. Xiao Li, Hua Shen and Hui Tan helped in synthesizing the probe used in this study. Yanli Li, Jie Xiao and Guobing Liu contributed to animal experiments. Jie Xiao, Xiaobo Xu, Dengfeng Cheng and Hongcheng Shi conceived and designed as well as controlled the quality of this study. All authors reviewed the manuscript.

**Conflicts of Interest:** All authors declare no conflict of interest.

## References

1. Siegel, R.L.; Miller, K.D.; Jemal, A. Cancer statistics, 2016. *CA Cancer J. Clin.* **2016**, *66*, 7–30. [[CrossRef](#)] [[PubMed](#)]
2. Gridelli, C.; Rossi, A.; Carbone, D.P.; Guarize, J.; Karachaliou, N.; Mok, T.; Petrella, F.; Spaggiari, L.; Rosell, R. Non-small-cell lung cancer. *Nat. Rev. Dis. Primers.* **2015**, *1*, 15009. [[CrossRef](#)] [[PubMed](#)]
3. Leighl, N.B. Treatment paradigms for patients with metastatic non-small-cell lung cancer: First-, second-, and third-line. *Curr. Oncol.* **2012**, *19*, S52–S58. [[CrossRef](#)] [[PubMed](#)]
4. Gerber, D.E.; Schiller, J.H. Maintenance chemotherapy for advanced non-small-cell lung cancer: New life for an old idea. *J. Clin. Oncol.* **2013**, *31*, 1009–1020. [[CrossRef](#)] [[PubMed](#)]
5. Folkman, J. Role of angiogenesis in tumor growth and metastasis. *Semin. Oncol.* **2002**, *29*, 15–18. [[CrossRef](#)] [[PubMed](#)]
6. Folkman, J. Tumor angiogenesis: Therapeutic implications. *N. Engl. J. Med.* **1971**, *285*, 1182–1186. [[PubMed](#)]
7. Hurwitz, H.; Fehrenbacher, L.; Novotny, W.; Cartwright, T.; Hainsworth, J.; Heim, W.; Berlin, J.; Baron, A.; Griffing, S.; Holmgren, E.; et al. Bevacizumab plus irinotecan, fluorouracil, and leucovorin for metastatic colorectal cancer. *N. Engl. J. Med.* **2004**, *350*, 2335–2342. [[CrossRef](#)] [[PubMed](#)]
8. Sandler, A.; Gray, R.; Perry, M.C.; Brahmer, J.; Schiller, J.H.; Dowlati, A.; Lilenbaum, R.; Johnson, D.H. Paclitaxel-carboplatin alone or with bevacizumab for non-small-cell lung cancer. *N. Engl. J. Med.* **2006**, *355*, 2442–2450. [[CrossRef](#)] [[PubMed](#)]
9. Larson, S.M.; Carrasquillo, J.A.; Cheung, N.V.; Press, O.W. Radioimmunotherapy of human tumours. *Nat. Rev. Cancer* **2015**, *15*, 347–360. [[CrossRef](#)] [[PubMed](#)]
10. Sahlin, M.; Bauden, M.P.; Andersson, R.; Ansari, D. Radioimmunotherapy—A potential novel tool for pancreatic cancer therapy? *Tumor. Biol.* **2015**, *36*, 4053–4062. [[CrossRef](#)] [[PubMed](#)]
11. Kawashima, H. Radioimmunotherapy: A Specific Treatment Protocol for Cancer by Cytotoxic Radioisotopes Conjugated to Antibodies. *Sci. World J.* **2014**, *2014*, 1–10. [[CrossRef](#)] [[PubMed](#)]
12. Grillo-Lopez, A.J. Zevalin: The first radioimmunotherapy approved for the treatment of lymphoma. *Expert Rev. Anticancer Ther.* **2002**, *2*, 485–493. [[CrossRef](#)] [[PubMed](#)]
13. Shadman, M.; Gopal, A.K.; Kammerer, B.; Becker, P.S.; Maloney, D.G.; Pender, B.; Shustov, A.R.; Press, O.W.; Pagel, J.M. Radioimmunotherapy consolidation using <sup>131</sup>I-tositumomab for patients with chronic lymphocytic leukemia or small lymphocytic lymphoma in first remission. *Leuk. Lymphoma* **2016**, *57*, 572–576. [[PubMed](#)]
14. Buchegger, F.; Larson, S.M.; Mach, J.P.; Chalandon, Y.; Dietrich, P.Y.; Cairoli, A.; Prior, J.O.; Romero, P.; Speiser, D.E. Radioimmunotherapy combined with maintenance anti-CD20 antibody may trigger long-term protective T cell immunity in follicular lymphoma patients. *Clin. Dev. Immunol.* **2013**, *2013*, 875343. [[CrossRef](#)] [[PubMed](#)]
15. Koechli, V.; Klaeser, B.; Banz, Y.; Mueller, B.U.; Pabst, T. Consolidation of first remission using radioimmunotherapy with yttrium-90-ibritumomab-tiuxetan in adult patients with *Burkitt lymphoma*. *Leuk. Res.* **2015**, *39*, 307–310. [[CrossRef](#)] [[PubMed](#)]
16. Kraeber-Bodere, F.; Bodet-Milin, C.; Rousseau, C.; Eugene, T.; Pallardy, A.; Frampas, E.; Carlier, T.; Ferrer, L.; Gaschet, J.; Davodeau, F.; et al. Radioimmunoconjugates for the treatment of cancer. *Semin. Oncol.* **2014**, *41*, 613–622. [[CrossRef](#)] [[PubMed](#)]
17. Lucas, S.; Feron, O.; Gallez, B.; Masereel, B.; Michiels, C.; Vander, B.T. Monte Carlo Calculation of Radioimmunotherapy with <sup>90</sup>Y-, <sup>177</sup>Lu-, <sup>131</sup>I-, <sup>124</sup>I-, and <sup>188</sup>Re-Nanoobjects: Choice of the Best Radionuclide for Solid Tumour Treatment by Using TCP and NTCP Concepts. *Comput. Math. Methods Med.* **2015**, *2015*, 284360. [[CrossRef](#)] [[PubMed](#)]
18. Lee, M.C.; Chung, J.K.; Lee, D.S.; Jeong, J.M.; Chang, Y.S.; Hong, M.K.; Yeo, J.S.; Lee, Y.J.; Kim, K.M.; Lee, S.J. In vitro properties and biodistribution of Tc-99m and Re-188 labeled monoclonal. *Korean. J. Nucl. Med.* **1998**, *6*, 516–524.
19. Sykes, T.R.; Somayaji, V.V.; Bier, S.; Woo, T.K.; Kwok, C.S.; Snieckus, V.; Noujaim, A.A. Radiolabeling of monoclonal antibody B43.13 with rhenium-188 for immunoradiotherapy. *Appl. Radiat. Isot.* **1997**, *48*, 899–906. [[CrossRef](#)]

20. De Decker, M.; Bacher, K.; Thierens, H.; Slegers, G.; Dierckx, R.A.; de Vos, F. In vitro and in vivo evaluation of direct rhenium-188-labeled anti-CD52 monoclonal antibody alemtuzumab for radioimmunotherapy of B-cell chronic lymphocytic leukemia. *Nucl. Med. Biol.* **2008**, *35*, 599–604. [[CrossRef](#)] [[PubMed](#)]
21. Wang, L.L.; Hu, R.C.; Dai, A.G.; Tan, S.X. Bevacizumab induces A549 cell apoptosis through the mechanism of endoplasmic reticulum stress in vitro. *Int. J. Clin. Exp. Pathol.* **2015**, *8*, 5291–5299. [[PubMed](#)]
22. Mukherji, S.K. Bevacizumab (Avastin). *Am. J. Neuroradiol.* **2010**, *31*, 235–236. [[CrossRef](#)] [[PubMed](#)]
23. Taylor, R.N.; Yu, J.; Torres, P.B.; Schickedanz, A.C.; Park, J.K.; Mueller, M.D.; Sidell, N. Mechanistic and therapeutic implications of angiogenesis in endometriosis. *Reprod. Sci.* **2009**, *16*, 140–146. [[CrossRef](#)] [[PubMed](#)]
24. Stein, R.; Govindan, S.V.; Chen, S.; Reed, L.D.; Richel, H.; Griffiths, G.L.; Hansen, H.J.; Godenberg, D.M. Radioimmunotherapy of a Human Lung Cancer Xenograft with Monoclonal Antibody RS7: Evaluation of <sup>177</sup>Lu and Comparison of Its Efficacy with That of <sup>90</sup>Y and Residualizing <sup>131</sup>I. *J. Nucl. Med.* **2001**, *42*, 967–974. [[PubMed](#)]
25. Griffiths, G.L.; Goldenberg, D.M.; Knapp, F.J.; Callahan, A.P.; Chang, C.H.; Hansen, H.J. Direct radiolabeling of monoclonal antibodies with generator-produced rhenium-188 for radioimmunotherapy: Labeling and animal biodistribution studies. *Cancer Res.* **1991**, *51*, 4594–4602. [[PubMed](#)]
26. Baidoo, K.E.; Lin, K.S.; Zhan, Y.; Finley, P.; Scheffel, U.; Wagner, H.N. Design, synthesis, and initial evaluation of high-affinity technetium bombesin analogues. *Bioconjug. Chem.* **1998**, *9*, 218–225. [[CrossRef](#)] [[PubMed](#)]
27. Winnard, P.J.; Chang, F.; Rusckowski, M.; Mardrossian, G.; Hnatowich, D.J. Preparation and use of NHS-MAG3 for technetium-99m labeling of DNA. *Nucl. Med. Biol.* **1997**, *24*, 425–432. [[CrossRef](#)]
28. Wang, Y.; Liu, X.; Hnatowich, D.J. An improved synthesis of NHS-MAG3 for conjugation and radiolabeling of biomolecules with <sup>99m</sup>Tc at room temperature. *Nat. Protoc.* **2007**, *2*, 972–978. [[CrossRef](#)] [[PubMed](#)]
29. Liu, G.; Hu, Y.; Xiao, J.; Li, X.; Li, Y.; Tan, H.; Zhao, Y.; Cheng, D.; Shi, H. <sup>99m</sup>Tc-labelled anti-CD11b SPECT/CT imaging allows detection of plaque destabilization tightly linked to inflammation. *Sci. Rep.* **2016**, *6*, 20900. [[CrossRef](#)] [[PubMed](#)]

**Sample Availability:** Samples of the compounds are not available from the authors.



© 2016 by the authors; licensee MDPI, Basel, Switzerland. This article is an open access article distributed under the terms and conditions of the Creative Commons Attribution (CC-BY) license (<http://creativecommons.org/licenses/by/4.0/>).